Published in final edited form as:
In Vivo. 2013 ; 27(5): 599–603.

A Clinically Relevant Mouse Model of Canine Osteosarcoma with Spontaneous Metastasis

Beth K Chaffee and
The Ohio State University, College of Veterinary Medicine, Columbus, OH, USA

Matthew J. Allen, Vet MB, Ph.D.
Department of Veterinary Clinical Sciences, College of Veterinary Medicine, The Ohio State University, 601 Vernon L. Tharp Street, Columbus, OH 43210, USA.

Abstract

Background/Aim—Many patients with osteosarcoma (OS) will succumb to distant metastasis, often involving the lungs. Effective therapies for treating lung metastases depend on the availability of a clinically relevant preclinical model.

Materials and Methods—Mice were surgically implanted with OS tumor fragments. The time course of primary tumor growth and subsequent spread to the lung were determined.

Results—Following development of a lytic and proliferative primary bone lesion, tumor metastasized to the lung in the majority of mice. There was no evidence of tumor at three weeks, but 10 out of 11 mice ultimately developed secondary OS in the lung within 12 weeks.

Conclusion—Implantation of OS tumor fragments leads to the development of primary bone tumors and secondary lung metastases, recapitulating the clinical behavior of OS. This model offers an advantage over cell suspension injection models by precluding initial seeding of the lung with tumor cells.

Keywords

Osteosarcoma; mouse model; metastasis

Osteosarcoma (OS) is the most common primary malignancy of bone in humans and the second most frequent cause of cancer-related death in children (1, 5). OS is also the most common primary bone tumor in dogs, most often affecting middle-aged to older large breeds. The incidence in the canine population is 10 times that of humans, with approximately 10,000 new cases per year in the United States. Furthermore, there are many similarities between human and canine OS including affected sites and gender predilection, association with increased height, and propensity for lung metastasis (8, 13, 14). Most cases of OS involve the metaphysis of long bones, with the distal femur, proximal tibia and proximal humerus being the most common sites in both species (3). The vast majority of OS are histologically high-grade and have a strong propensity to metastasize.

Correspondence to: Beth K. Chaffee Medicine, The Ohio State University, D.V.M., DACVP, Department of Veterinary Biosciences, College of Veterinary 6142927237, chaffee.15@osu.edu.

Despite improvements in the management of the primary bone disease associated with OS (2), many human and veterinary patients will eventually succumb to distant metastasis, most often involving the lungs. At the time of diagnosis, fewer than 20% of patients have clinically detectable metastases; however, over 80% have micrometastases at the time of diagnosis as shown by distant recurrence of the tumor following resection of the primary mass (6).

In order to reduce the morbidity and mortality associated with OS, it is critical to address the issue of lung metastasis. Metastasis is a complex process with numerous steps involved (15). Although a number of canine, human and murine OS cell lines have been characterized *in vitro* and *in vivo* (4, 8), a widely accepted orthotopic mouse model of OS with reliable metastasis has not yet been established. One commonly used technique to study OS involves injection of an OS cell suspension into the femur or tibia of the mouse. In pilot studies using the Abrams canine OS cell line, we identified a number of animals that died acutely following intratibial injection of tumor cells. At necropsy, these mice had microscopic evidence of tumor micro-emboli within the pulmonary vasculature. In addition, acute removal of the primary bone lesion, by amputation, did not result in a reduction in the incidence or severity of lung pathology, nor in a change in overall survival. These results indicate that this model did not replicate the complete metastatic cascade in all cases, and so we set out to develop a more clinically relevant model of OS.

We elected to continue to use the Abrams cell line for this work because of its aggressive biological behavior and clinical relevance in terms of tissue tropism (8, 11). To avoid potential concerns over embolization of a cell suspension, solid fragments of Abrams tumor were transplanted orthotopically into the medullary canal of the proximal tibia. The temporal patterns of tumor growth at the primary site were evaluated by radiography and histology, and the incidence and severity of subsequent secondary OS development in the lungs was quantified using stereological analysis of histological sections.

Material and Methods

Cell culture

The Abrams canine OS cell line was kindly provided by Dr. Doug Thamm, (College of Veterinary Medicine & Biomedical Science, Colorado State University). Cells were cultured in Dulbecco's modified Eagle's medium (DMEM) (Gibco, Grand Island, NY, USA) supplemented with 10% fetal calf serum (FCS) (HyClone, Logan, UT, USA) and 1% penicillin/streptomycin (Gibco). Vented tissue culture flasks (Corning Life Sciences, Corning, NY, USA) were maintained at 37°C in a humidified atmosphere of 5% carbon dioxide in air, and cells were split when they reached approximately 80-90% confluency.

Animals

All animal study procedures and protocols were conducted with approval of the Institutional Animal Care and Use Committee (#2008A0062-R1). Female, 4-5 week old, BALB/c *Foxn1 nu/nu* mice (Taconic Farms, Germantown, NY, USA) were housed 4-5 animals per cage. All surgical procedures were performed under sterile conditions.

Subcutaneous tumor growth

Abrams cells were harvested and resuspended in sterile phosphate-buffered saline (PBS) at a density of 10^7cells/ml. Trypan blue staining was used to verify a minimum of 90% cell viability before and after the procedure. Mice were anesthetized and 0.15 ml of the cell suspension was injected subcutaneously over the right thigh. Mice were weighed weekly and tumor size was monitored. After four weeks the mice were euthanized and the tumors were harvested aseptically. Tumor tissue was minced into multiple small fragments and bathed in warm supplemented DMEM (as described above) until implanted, or cryopreserved in DMEM containing 20% FCS and 10% dimethyl sulfoxide (DMSO). Cryopreserved tissues were frozen under controlled conditions using a commercial cryopreservation system (Nalgene Thermo-Scientific, Rochester, NY, USA) at - 80°C and then stored in liquid nitrogen. Additional tumor fragments were snap frozen by immediately immersing them in liquid nitrogen and stored at -80°C.

Surgical implantation of tumor fragments

Freshly harvested or previously frozen fragments of Abrams tumor tissue were immersed in warm DMEM. Mice were anesthetized and the right hind limb scrubbed with surgical antiseptic. The skin was incised to expose the medial tibial cortex, and a small hole was made through the cortex. Multiple small fragments of solid tumor tissue (totaling approximately 0.5 mm^3 of tissue) were inserted into the medullary cavity of the tibia. The skin edges were then apposed with liquid tissue adhesive (3M, St. Paul, MN, USA).

Tibial tumor growth was monitored by weekly digital microradiographs (Model LX-60; Faxitron) using an exposure time of 5 s at 30kV. In addition mice were weighed weekly and examined for signs of ill-thrift, lameness or swelling around the surgical site. All mice underwent amputation of the affected limb after five weeks. The amputated limbs were fixed in 10% formalin and then decalcified in 10% EDTA and submitted for routine histology. Twelve weeks following intratibial injection of tumor cells or after a 20% loss in body weight (whichever came first), mice were euthanized. A complete necropsy was performed by a veterinary pathologist to look for metastases. The lungs were inflated with formalin, immersion fixed in formalin for at least 48 hours and then processed for stereologic analysis (see below).

Hind limb amputation

Mice were anesthetized and the right hind limb was disinfected. A circumferential elliptical incision around the mid-thigh was made and the skin and were reflected. A stainless steel ligating clip (Ethicon Endo-surgery, Blue Ash, OH, USA) was used to ligate the femoral artery. The thigh muscles were transected between the two clips and reflected off of the proximal aspect of the femur. The coxofemoral joint capsule was transected to free the femoral head. The cut end of the sciatic nerve was anesthetized with lidocaine and the muscles of the hip region were sutured over the acetabulum. The skin incision was closed with intradermal sutures and reinforced with tissue adhesive. Postoperatively, mice were treated with buprenorphine and meloxicam for three days.

Tissue collection, processing and stereological analysis

Formalin-inflated lungs were embedded in a 3% agar solution (Fisher Scientific, Fair Lawn, NJ, USA) that was allowed to set at 20°C overnight. A tissue-sampling matrix (Zivic Instruments, Pittsburgh, PA, USA) was used to generate random uniform sections at 2-mm increments through the entire volume of the lung tissue. Each slice was then routinely processed and a standardized sectioning protocol was used for each block. Bioquant Image Analysis Software (Nashville, TN, USA) was used to manually quantify total lung area and lung area effaced by tumor. These numbers were used to calculate the percentage of lung (lung area affected by tumor/total lung area x100) that contained OS tumor tissue in each mouse (21).

Results

Surgical implantation technique

A preliminary feasibility study was performed using five mice implanted with fragments of fresh Abrams tumor derived from a solid tumor grown subcutaneously in a donor mouse. All five recipients developed primary OS lesions in the tibia. Radiographic changes (bone destruction with some new bone formation) progressed rapidly (Figure 1) until they required amputation at five weeks post-implantation.

Microscopically, the primary lesions in the tibia were characterized by large areas of bone destruction associated with an expansile intramedullary mass of neoplastic osteoblasts displaying marked anisocytosis, cellular atypia, a high mitotic index and central necrosis (Figure 2). All five mice survived to 12 weeks post-implantation, at which point four out of five mice (80%) had gross and microscopic evidence of lung metastasis (Figure 3). Lung lesions were characterized by multifocal, variably-sized nodules composed of neoplastic osteoblasts, sometimes producing an osteoid-like matrix and displaying marked anisocytosis, a high mitotic rate and prominent central necrosis, very similar to the primary bone lesions (Figure 4). One mouse at the 12-week end point did not have any evidence of metastasis.

In the main experiment, we sought to characterize the development of the primary bone lesion, quantify metastasis and examine the possibility of utilizing cryopreserved tumor tissue. Fifteen mice were implanted with fresh tumor tissue and two mice were euthanized each week (up until amputation at five weeks) to examine the time course of primary and metastatic tumor development. At five weeks post-implantation the remaining mice that had developed primary bone lesions underwent right hind limb amputation and were monitored for an additional 12 weeks. In parallel with this, another group of five mice were implanted with cryopreserved tumor fragments. Mice that developed a primary bone lesion were amputated at five weeks post-implantation and monitored for 12 weeks. Finally, a group of five mice were implanted with snap-frozen tumor tissue. None of the mice in this group developed any evidence of primary or metastatic tumors after 12 weeks.

Radiography of the tibias at different time points showed progressive tumor growth and destruction of pre-existing tibial cortex with formation of new neoplastic and reactive bone. None of the mice euthanized prior to three weeks had any evidence of lung metastasis. One

out of two mice euthanized at three weeks and at four weeks had lung metastases, but a minimal percentage of the lung volume was affected (0.04% and 0.03% respectively). Of the six mice with confirmed primary tumors (including four implanted with cryopreserved tissue), all six had metastasis to the lung at the time of euthanasia. Lungs from these mice were analyzed and the mean percentage of affected lung was 33.4% ± 24.3%.

Discussion

OS continues to be a devastating diagnosis due to the young age of the patients and the high rate of metastases. Over 80% of human patients are believed to have microscopic metastases at the time of diagnosis (6). The same can be said for metastatic disease in canine patients (12). For these reasons, it is critically important to have a clinically relevant mouse model that can be used to investigate the molecular mechanisms of metastasis and to evaluate novel therapeutic agents, with a focus on preventing or reducing metastatic burden. Given the similarities in the biology of the disease in humans and in dogs, we anticipate that knowledge gained from studies on either species will translate into clinical benefits for both.

Prior to starting the experiments reported here, we had evidence of tumor micro-embolization following intratibial injection of Abrams cells. On this basis, we elected to focus on the development of a more clinically relevant model for our subsequent studies. While the surgical implantation technique proved to be more technically challenging than the injection technique, the use of intact tissue fragments precluded the possibility of tumor embolization following the initial tumor implantation. None of the mice implanted with tumor developed lung metastasis earlier than three weeks. These results contrast starkly with those from the intratibial injection model, in which there was early development of lung lesions that progressed rapidly. The solid fragment technique proved equally successful with fresh or carefully cryopreserved tissue; as expected, snap-frozen tissue did not maintain adequate viability to grow once implanted. The growth of the tumor at the primary site in bone, followed by amputation and later, a high rate of lung metastasis, successfully recapitulates the typical clinical disease course in humans and dogs. The reliable occurrence of true spontaneous lung metastasis from a primary bone tumor in this model allows us to investigate individual steps in the metastatic cascade and identify potential therapeutic targets.

This model also allows us to evaluate primary canine and human OS tumor samples by directly implanting them into an orthotopic site in a mouse model while components of the original tumor microenvironment, without the need for *in-vitro* growth. Multiple studies have shown that protein and gene expression levels can be significantly *in-vitro versus in-vivo* growth, not to mention the varied conditions under which cells might be grown *in vitro* (9, 10). Utilizing this model we will be better equipped to investigate the factors contributing to metastasis and, ultimately, to develop therapeutic strategies that will improve the prognosis for canine and human patients diagnosed with OS. Furthermore, as we move towards a more personalized approach to diagnosis and treatment (7), the model will facilitate comparison of different therapeutic regimens against a patient's specific tumor and may be predictive of the patient's response to therapy.

Acknowledgments

The Authors acknowledge Feng Xu for her assistance with the animal experiments and Dr. Krista La Perle for critical review of the manuscript. The project described was supported in part by grant number 8UL1TR000090-05 from the National Center for Advancing Translational Sciences. The content is solely the responsibility of the Authors and does not necessarily represent the official views of the National Center for Advancing Translational Sciences or the National Institutes of Health.

References

1. Arndt CA, Rose PS, Folpe AL, Laack NN. Common musculoskeletal tumors of childhood and adolescence. Mayo Clin Proc. 2012; 87:475–487. [PubMed: 22560526]
2. Bacci G, Ferrari S, Mercuri M, Bertoni F, Picci P, Manfrini M, Gasbarrini A, Forni C, Cesari M, Campanacci M. Predictive factors for local recurrence in osteosarcoma: 540 patients with extremity tumors followed for minimum 2.5 years after neoadjuvant chemotherapy. Acta Orthop Scand. 1998; 69:230–236. [PubMed: 9703394]
3. Chun R, de Lorimier L. Update on the biology and management of canine osteosarcoma. Vet Clin North Am Small Anim Pract. 2003; 33:491–516. [PubMed: 12852233]
4. Dass CR, Ek ET, Choong PF. Human xenograft osteosarcoma models with spontaneous metastasis in mice: clinical relevance and applicability for drug testing. J Cancer Res Clin Oncol. 2007; 133:193–198. [PubMed: 17031670]
5. Fan TM. Animal models of osteosarcoma. Expert Rev Anticancer Ther. 2010; 10:1327–1338. [PubMed: 20735317]
6. Ferguson WS, Goorin AM. Current treatment of osteosarcoma. Cancer Invest. 2001; 19:292–315. [PubMed: 11338887]
7. Hamilton SR. Molecular pathology. Mol Oncol. 2012; 6:177–181. [PubMed: 22516585]
8. Legare ME, Bush J, Ashley AK, Kato T, Hanneman WH. Cellular and phenotypic characterization of canine osteosarcoma cell lines. J Cancer. 2011; 2:262–270. [PubMed: 21552385]
9. Lisle JW, Choi JY, Horton JA, Allen MJ, Damron TA. Metastatic osteosarcoma gene expression differs in vitro and in vivo. Clin Orthop Relat Res. 2008; 466:2071–2080. [PubMed: 18516656]
10. Lund S, Christensen KV, Hedtjärn M, Mortensen AL, Hagberg H, Falsig J, Hasseldam H, Schrattenholz A, Pörzgen P, Leist M. The dynamics of the LPS triggered inflammatory response of murine microglia under different culture and in vivo conditions. J Neuroimmunol. 2006; 180:71–87. [PubMed: 16996144]
11. MacEwen EG, Pastor J, Kutzke J, Tsan R, Kurzman ID, Thamm DH, Wilson M, Radinsky R. IGF-1 receptor contributes to the malignant phenotype in human and canine osteosarcoma. J Cell Biochem. 2004; 92:77–91. [PubMed: 15095405]
12. Morello E, Martano M, Buracco P. Biology, diagnosis and treatment of canine appendicular osteosarcoma: Similarities and differences with human osteosarcoma. Vet J. 2010
13. Mueller F, Fuchs B, Kaser-Hotz B. Comparative biology of human and canine osteosarcoma. Anticancer Res. 2007; 27:155–164. [PubMed: 17352227]
14. Withrow SJ, Powers BE, Straw RC, Wilkins RM. Comparative aspects of osteosarcoma. Dog versus man. Clin Orthop Relat Res. 1991:159–168.
15. Woodhouse EC, Chuaqui RF, Liotta LA. General mechanisms of metastasis. Cancer. 1997; 80:1529–1537. [PubMed: 9362419]

Figure 1.

Sequential radiographs of a mouse surgically implanted with solid osteosarcoma fragments. Radiographs were taken at weekly intervals until amputation at 5 weeks post-postoperatively. Note progressive osteolysis and neoplastic new bone formation.

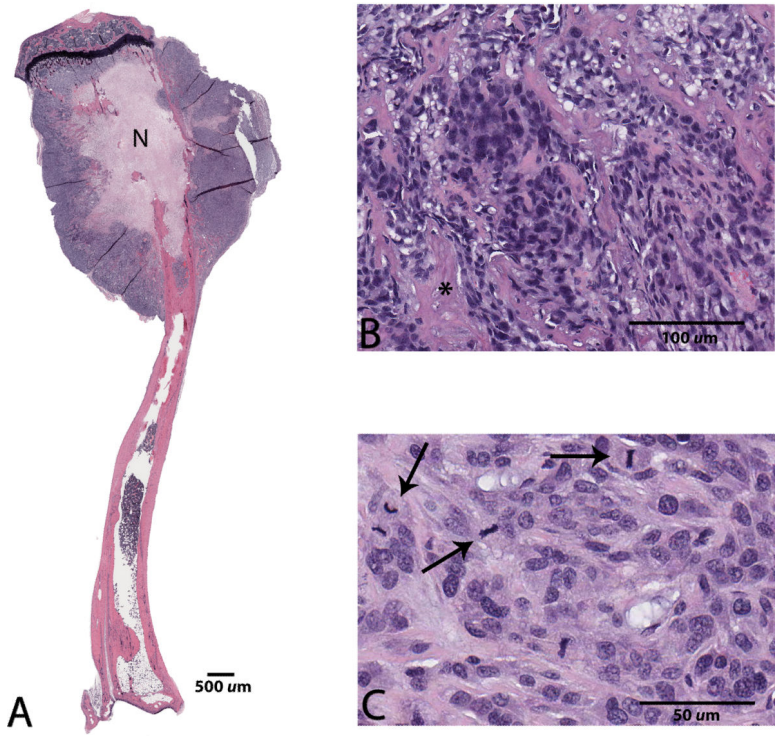

Figure 2.

Photomicrographs of a tibial osteosarcoma lesion five weeks following surgical implantation of solid tumor tissue. A: Note the bone destruction by neoplastic osteoblasts, and central coagulation necrosis (N), x0.5 magnification. B,C: At higher magnification, neoplastic cells display osteoid production (asterisk), marked anisocytosis, cellular atypia, and numerous mitotic figures (arrows), x20 and x40 magnification, respectively. Hematoxylin and eosin staining.

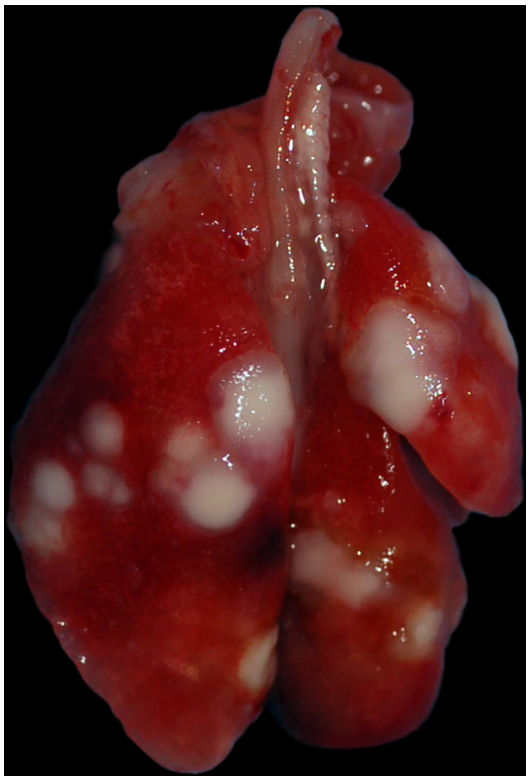

Figure 3.

Macroscopic appearance of multiple lung metastases in a mouse 12 weeks after undergoing surgical implantation of solid osteosarcoma tumor fragments.

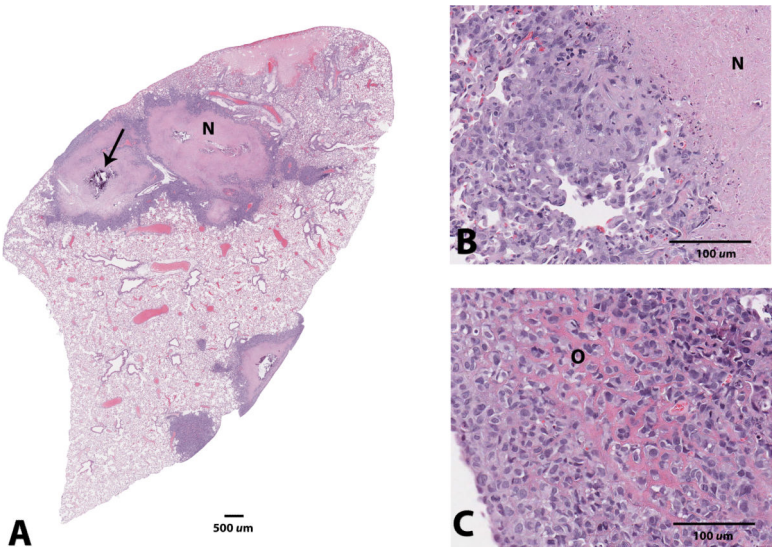

Figure 4.

Photomicrographs of the lung metastases in a mouse 12 weeks after undergoing surgical implantation of solid osteosarcoma tumor fragments. A: Variably-sized nodules composed of neoplastic osteoblasts surrounding a central region of coagulation necrosis (N) with occasional dystrophic mineralization (arrow), x0.5 magnification. B,C: Higher magnification of the coagulation necrosis (N); some neoplastic cells produce eosinophilic, osteoid-like matrix (O), x20 magnification. Hematoxylin and eosin staining.